Influence of pre-existing volcanic edifice geometry on caldera formation

Virginie Pinel

Influence of pre-existing volcanic edifice geometry on caldera formation

V. Pinel,[1]

V. Pinel, ISTerre, IRD R219, CNRS Université de Savoie, Campus Scientifique, 73376 Le Bourget du Lac Cedex, France (Virginie.Pinel@univ-savoie.fr)

[1] ISTerre, IRD R219, CNRS Université de Savoie, Campus Scientifique, 73376 Le Bourget du Lac Cedex, France

Abstract. Volcanic edifice construction at the Earth's surface significantly modifies the stress field within the underlying crust with two main implications for caldera formation. First, tensile rupture at the Earth's surface is favored at the periphery, which enables ring fault formation. Second, edifice formation amplifies the amount of pressure decrease occurring within a magma reservoir before the eruption stops. Taking into account both of these effects, caldera formation can be initiated during a central eruption of a pre-existing volcano even when assuming elastic behaviour for the surrounding crust. Providing the roof aspect ratio is small enough, conditions for caldera formation by reservoir withdrawal can be reached whatever the reservoir shape is. However ring fault initiation is easier for laterally elongated reservoirs.

1. Introduction

Many caldera-forming deposits record energetic eruptive phases prior to the "syncollapse" deposits characterized by ignimbrites, which is consistent with an onset of caldera occurring during an ongoing eruption that is to say when the magma reservoir pressure is decreasing by withdrawal [*Marti et al.*, 2008]. Based on this field observation as well as experimental and mathematical modelling, *Marti et al.* [2009] define two types of caldera depending on the pressure evolution within the magmatic reservoir leading to ring faults formation and caldera-forming eruption. One caldera type is formed by magma pressure increase within a sill-like magma reservoir in the presence of a regional extensive field [*Gudmundsson*, 1998] and starts with the eruption. The other caldera type is formed by magma pressure decrease during an ongoing eruption. Based on the compilation of information gathered in the Collapse Caldera Data Base (CCDB), *Geyer and Marti* [2008] show that the second type that occurs during reservoir withdrawal is, by far, the most common.

In the case of caldera formation induced by reservoir withdrawal, the key question to address, concerns the amount of depressurization that a given reservoir can reach and whether or not this depressurization is sufficient to ensure ring fault formation. Considering the crustal surrounding medium as elastic, reservoir depressurization is limited by dyke closure at the reservoir wall [*McLeod and Tait*, 1999; *Marti et al.*, 2008]. However, except for a few recent studies [*Geyer et al.*, 2006; *Folch and Marti*, 2009], most of theoretical work based on fluid dynamics [*Druitt and Sparks*, 1984], as well as analogical [*Roche et al.*, 2000] and numerical studies [*Folch and Marti*, 2004] ignore this problem

and do not discuss whether or not conditions for ring fault initiation are compatible with realistic pressure conditions within the reservoir. Besides, most authors favoring caldera formation by reservoir withdrawal consider that the crust has to behave non-elastically [*Marti et al.*, 2008].

The fact that caldera characteristics are linked to the pre-existing volcanic edifice geometry has long been recognised [*Wood*, 1984]. More recently, based on the compilation of information gathered in the Collapse Caldera Data Base (CCDB), *Geyer and Marti* [2008] showed that, in most cases ($53,3\%$) pre-caldera volcanic activity involves the development of long lived stratovolcanoes or stratocones and that another significant amount (11%) of calderas are formed on pre-existing shield volcanoes. It is known that eruptive products accumulation at the Earth's surface and edifice formation significantly modifies the underlying stress field within the crust with consequences for the magma plumbing system development [*Pinel and Jaupart*, 2003]. However only a few studies dealing with caldera formation take into account the edifice's potential influence [*Walter and Troll*, 2001; *Lavallée et al.*, 2004; *Pinel and Jaupart*, 2005].

In this study, numerical simulations in axisymmetric geometry are performed in order to determine under which conditions a caldera formation might occur when considering a realistic range of pressure within the magma reservoir and a volcanic edifice at the Earth's surface. The model is developed following the framework proposed by *Pinel and Jaupart* [2005] who performed an analytical study in 2D (plane strain approximation) for cylindrical magma reservoirs. In this new paper, the influence of the roof aspect ratio (reservoir depth/reservoir lateral extension), the reservoir size as well as the edifice slope

are discussed, and a primary additional contribution is to investigate the influence of the reservoir shape (ellipticity).

2. Model description

2.1. Geometry and general settings

An ellipsoidal magma reservoir filled with liquid magma embedded in an homogeneous elastic medium (rigidity G and Poisson's ratio ν) is considered (see Fig 1 a). The magma density is assumed equal to the density (ρ) of the surrounding crust and the state of reference is lithostatic ($\sigma_{rr} = \sigma_{zz} = \sigma_{\theta\theta} = -\rho g z > 0$ with $-z$, the depth). Departure from this lithostatic state of reference is induced by either a differential magma pressure ($\Delta P > 0$ for an overpressurized reservoir and $\Delta P < 0$ for an underpressurized reservoir) or the presence of an edifice at the Earth's surface, whose geometry is characterized by its radius R_v and slope α. The magma reservoir geometry is characterized by its horizontal semi-axis a, its vertical semi-axis b and its roof depth H. A key parameter is the reservoir ellipticity (e) defined by the ratio $e = a/b$, ellipticity being equal to 1 for the spherical case, smaller than 1 for vertically elongated reservoirs (prolate) and larger than 1 for horizontally elongated reservoirs (oblate). The maximum value of the semi-axis will be referred to as L_c ($L_c = a$ for oblate shapes and $L_c = b$ for prolate ones). Another key parameter when studying calderas is the roof aspect ratio (R) defined as the ratio of the reservoir roof thickness over its width ($R = H/(2a)$) [*Roche et al.*, 2000; *Geyer et al.*, 2006].

Stress and strain within the crust are numerically calculated solving the equations for linear elasticity with the "Finite Element Method" (COMSOL software). The domain of calculation is a 100*100 km square box with a mesh of about 100 000 triangular units that

is refined around the volcanic edifice and magma reservoir. No displacement perpendicular to the boundary is allowed at the bottom and lateral boundaries, the upper boundary is considered as a free surface. The edifice is modelled with a normal stress applied at the upper surface ($\sigma_n = \rho_m g \alpha R_v(1 - r/R_v)$ for $r < R_v$) and a normal stress equal to the magma overpressure is applied at the reservoir walls. Numerical solutions have been validated using well-known analytical solutions as detailled in *Albino et al.* [2010]. Figure 1b shows that the edifice load at the surface tends to induce, respectively, compression in the central part, and tension at the periphery, the tensile effect having a smaller amplitude. An underpressurized reservoir has roughly the same effect (Fig. 1c) whereas the effect of an overpressurized reservoir (Fig. 1d) is opposite (large tensile stress in the central part and comparatively small compressive stress at the periphery).

2.2. Condition for caldera formation

Most numerical studies consider that the main criterion required for caldera formation is that tensile failure can occur at the Earth's surface at some lateral distance from the axis in order to produce ring faults [*Gudmundsson et al.*, 1997; *Folch and Marti*, 2004; *Pinel and Jaupart*, 2005]. It is also often required for the rupture location to be above the maximum lateral extension of the underlying magma reservoir [*Folch and Marti*, 2004; *Kinvig et al.*, 2009] to ensure the mechanical behaviour of the ring fault linking the Earth's surface to the reservoir walls and to reproduce field observations. For a detailled description of conditions required for ring faults formation see *Folch and Marti* [2004]; *Kinvig et al.* [2009]; *Geyer and Binderman* [2011].

Here, the criterion considered for caldera formation only requires that tensile failure of the Earth's surface occurs at some distance from the axis. However the position of this

rupture with regards to the reservoir walls is discussed later.

Tensile failure of the Earth's surface periphery should be favored by the edifice load (Fig. 1b) and the reservoir depressurization (Fig. 1c). The tensile failure criterion given by *Pinel and Jaupart* [2005] is generalised here in the three-dimensions, in order to calculate the magma pressure required within the reservoir for roof breakdown. It follows that tensile rupture occurs when $[2\sigma_{rr}(r, z = 0) - \sigma_{zz}(r, z = 0) - \sigma_{\theta\theta}(r, z = 0)]/3 = -T_s$, where σ_{rr}, σ_{zz} and $\sigma_{\theta\theta}$ are the three principal components of the stress tensor at the Earth's surface expressed in the cylindrical coordinate system, and T_s is the rock tensile strength. Due to the tensile effect, respectively, induced by an overpressurized reservoir in the central part (see Figure 1 d), and an underpressurized reservoir at the periphery (see Figure 1 c), tensile rupture induced by reservoir inflation only occurs at the axis (r=0) and cannot account for ring fault formation. Earth's surface rupture at the periphery is thus the consequence of reservoir pressure decrease (reservoir deflation) below a threshold value (ΔP_{crit}), such that the above equation is verified.

2.3. Realistic pressure range within the reservoir

Magma pressure within a reservoir might increase by replenishment and/or by volatiles exsolution due to magma crystallisation [*Tait et al.*, 1989]. However this increase is limited by the rupture of the reservoir walls leading to magma propagation away from the reservoir. Failure of the reservoir wall occurs when the deviatoric stress component, at the walls, reaches the tensile strength [*Tait et al.*, 1989; *Pinel and Jaupart*, 2003]. When magma leaves the reservoir, it induces a pressure decrease within the storage zone. Considering an elastic behaviour of the crust, this pressure decrease is also limited. When the magma pressure fails below the normal pressure applied at the dyke walls, the dykes get

closed. Conditions for the cessation of magma withdrawal define a lower bound for the reservoir pressure noted ΔP_{min}. One must assess whether or not the pressure decrease within the magma reservoir can be sufficient to induce ring fault formation, that is to say that we have to specify conditions under which one may have $\Delta P_{min} < \Delta P_{crit}$.

3. Results

Figure 2 shows, for various reservoir ellipticities, the edifice size required for caldera formation (to have $\Delta P_{min} < \Delta P_{crit}$). Within the framework of this particular model, which considers an initial lithostatic stress field, ring fault formation is not expected, when no edifice is present at the Earth's surface, whatever the reservoir shape is. The edifice growth at the surface always acts to favor tensile rupture at the periphery and, in most case, enables the reservoir to becomes underpressurized ($\Delta P_{min} < 0$) [*Pinel et al.*, 2010]. Both effects tend to favor ring faults formation. In the case of a roof aspect ratio equal to 1, caldera formation can only occur for horizontally elongated reservoirs, whereas, when the roof aspect ratio is equal to 0.25, caldera formation might occur whatever the reservoir shape is, the edifice size required being larger for prolate reservoirs. Results previously obtained in 2D by *Pinel and Jaupart* [2005] are similar to this paper's new results in 3D when considering a spherical shape, except for a small reservoir (Fig. 2 a), for which ring fault initiation appears more difficult in 2D. Figure 2 also shows that the fault linking the Earth's surface rupture to the reservoir wall is nearly vertical only for small roof aspect ratios. For a given reservoir ellipticity, the edifice size required for caldera formation usually increases with the roof aspect ratio. For a strato-volcano characterized by a slope of 30 degrees, the maximum roof aspect ratio allowing caldera formation is close to 1 and I checked that this maximum value does not evolve when considering larger

ellipticities.

In order to interpret field observations, it might be useful to compare the caldera and edifice predicted sizes. Figure 3 shows that, in general, the caldera is smaller than the pre-existing edifice (caldera/edifice radius smaller than 1). The amount of the edifice surface affected by the caldera collapse increases with the magma reservoir size (larger values of caldera/edifice radius for plain curves than for dotted ones). Another observation is that the caldera accounts for a larger fraction of the edifice in stratovolcanoes ($\alpha > 0.3$, Fig 3a,b) than in shield volcanoes ($\alpha \approx 0.1$, Fig 3c), which is consistent with field observations [*Wood*, 1984]. The caldera versus edifice ratio can bring additional constraints on the magma reservoir shape and size. Information on caldera geometry is available in most cases from the CCDB whereas the volcanic edifice size can be inferred from the topography provided by the SRTM Digital Elevation Model. In a few cases, the CCBD also provides an estimation of the roof aspect ratio. Such data have been reported for seven volcanoes to Figure 3. For instance, Crater Lake caldera formed on Mount Mazama, 6845 yr ago, is characterized by an edifice slope close to 0.3, a caldera versus edifice radius of 0.4 [*Pinel and Jaupart*, 2005] and a roof aspect ratio between 0.5 and 1. From Figure 3 b), this geometry is consistent with a 4 km radius spherical reservoir or a smaller reservoir (2.5 km radius) as previously proposed by *Pinel and Jaupart* [2005] but having a laterally elongated shape. Vesuvius is characterized by a slighly larger caldera/edifice radius (around 0.5) as well as a slighly larger roof aspect ratio (between 0.6 and 1.2), which is consistent with a 4km radius laterally elongated reservoir. An oblate shape is thus required for the magma reservoir at Vesuvius, as previously proposed by *Pinel and Jaupart* [2005]. From Figure 3 c) the formation of Medecine Lake or Newberry calderas, on pre-existing shield

volcanoes could be explained by the presence of a very shallow reservoir of radius 2.5 km or a slightly larger and deeper one (radius around 4km), whereas the formation of Opala, Ksudach and Krashennikov calderas in Kamchatka can only be explained by shallow and large spherical reservoirs ($L_c \geq 4km$).

4. Discussion and Conclusion

In order to explain caldera formation by magma withdrawal, *Marti et al.* [2008] consider that the reservoir wall behaviour departs from elasticity. Some phenomena such as conduit wall erosion could eventually prevent dyke from closure. However erosion of the central conduit by respectively, abrasion or fluid shear stress, is mainly restricted to a limited portion, respectively, above or around, the fragmentation level [*Macedonio et al.*, 1994], which is supposed to be located within the upper 1 km of the conduit [*Massol and Koyaguchi*, 2005]. It follows that, in most cases, it seems realistic to neglect conduit wall erosion at the magma reservoir level, before ring faults formation. The main conclusion of the present study is that caldera formation by reservoir withdrawal (that is to say, pressure decrease) can occur even considering an elastic behaviour for the surrounding crust. However, in order to further discuss the potential effects of previous events, lateral variations of the physical properties of the crust should be taken into account.

This study based on an elastic model only allows discussion of the initiation of caldera formation that is to say the onset of medium fracturation. It does not bring any insight into the further development of the caldera and the way the initial fracture propagates, which would require analog modelling [*Roche et al.*, 2000] or the use of numerical modelling based on the Discrete Element Method (DEM) [*Hardy*, 2008; *Holohan et al.*, 2009]. Once the

caldera formation has started the crustal behaviour can obviously no longer be considered as elastic.

This work only considers caldera formation associated with a summit eruption. Some caldera formations, mainly in the case of basaltic volcanoes, are caused by lateral eruptions or magma intrusions [*Michon et al.*, 2011]. Lateral magma propagation as well as often associated large flank displacements, indicate an extensional regime within the edifice. It follows that the model presented here, which relies on the assumption of an initial lithostatic stress field, is not appropriated to discuss such cases.

This study shows that the building of a volcanic edifice by accumulation of eruptive products at the Earth's surface favors caldera formation by inducing tensile stress at the Earth's surface and enabling larger depressurization within the magma reservoir. This conclusion was already supported by an earlier analytical study [*Pinel and Jaupart*, 2005] however it is, here, generalised for the 3-dimensional case and various reservoir shapes. Conditions for coherent caldera formation are easier to achieve in the case of small roof aspect ratios, as shown by *Roche et al.* [2000]; *Pinel and Jaupart* [2005]; *Geyer et al.* [2006]. For larger roof aspect ratios, larger edifice size are required to induce caldera formation. Caldera collapse can even affect vertically elongated reservoirs provided that the roof aspect ratio remains small. However horizontally elongated reservoir are much more favorable. With this particular geometry, caldera formation might occur for larger roof aspect ratios. The present model considering an initial lithostatic stress field cannot explain caldera formation in the case where there is no pre-existing edifice at the Earth's surface (which represents less than 15% of the documented calderas as reported by the CCDB *Geyer and Marti* [2008]) or if the roof aspect ratio is larger than 1 for stratovol-

canoes or larger than 1.3 for shield volcanoes (which represents a few documented cases, for example Ceburoco, as reported by the CCDB). It can also not explain ring fault initiation by reservoir inflation. However the initial stress field could be, in many cases, different from the lithostatic one and most calderas are formed in extensional tectonic regime (which is the case for Ceboruco). The effect of an extensional regime should favor caldera formation and could be easily quantified with the framework used in this study. The model presented here predicts that the caldera size versus the edifice one should be smaller in case of shield volcanoes than for strato-volcanoes, which is consistent with observations [*Wood*, 1984]. It also places some constraints on the magma reservoir geometry based on surface observations.

Acknowledgments. The author thanks F. Albino for his help with numerical modelling development, J. Marti and A. Geyer for providing helpful comments.

References

Albino, F. and Pinel, V. and Sigmundsson, F. (2010),Influence of surface load variations on eruption likelihood: Application to two Icelandic subglacial volcanoes, Grimsvötn and Katla, *Geophys. J. Int.*, *181*, 1,510–1,524.

Druitt, T. H., and R. S. J. Sparks (1984), On the formation of calderas during ignimbrite eruptions, *Nature*, *310*, 679–681.

Folch, A., and J. Marti (2004), Geometrical and mechanical constraints on the formation of ring-fault calderas, *Earth Planet. Sci. Lett.*, *221*, 215–225.

Folch, A., and J. Marti (2009), Time-dependent chamber and vent conditions during explosive caldera-forming eruptions, *Earth Planet. Sci. Lett.*, *280*, 246–253.

Geyer, A., and J. Marti (2008), The new worldwide collapse caldera database (ccdb): A tool for studying and understanding caldera processes, *J. Volcanol. Geotherm. Res.*, *175*, 334–354.

Geyer, A., A. Folch, and J. Marti (2006), Relationship between caldera collapse and magma chamber withdrawal: an experimental approach, *J. Volcanol. Geotherm. Res.*, *157*, 375–386.

Geyer, A., I. Binderman, Glacial influence on caldera-forming eruptions, *J. Volcanol. Geotherm. Res.*, *in press*.

Gudmundsson, A. (1998), Formation and development of normal-fault calderas and the initiation of large explosive eruptions, *Bull. Volcanol.*, *60*, 160–170.

Gudmundsson, A., J. Marti, and E. Turon (1997), Stress fields generating ring faults in volcanoes, *Geophysical Research Letters*, *24*, 1,559–1,562.

Hardy, S. (2008), Structural evolution of calderas: Insights from two-dimensional discrete element simulations, *Geology*, *36*, 927–930.

Holohan, E. P., M. P. Schöpfer, and J. J. Walsh (2009), Pit Craters and Collapse Calderas: Structural Influences of Initial Mechanical and Geometric Properties as revealed by 2D Distinct Element Method (DEM) Models, *Eos. Trans. AGU*, *90*.

Kinvig, H. S., A. Geyer, and J. Gottsmann (2009), On the effect of crustal layering on ring-fault initiation and the formation of collapse calderas, *J. Volcanol. Geotherm. Res.*, *186*, 293–304.

Lavallée, Y., J. Stix, B. Kennedy, M. Richer, and M.-A. Longpré (2004), Caldera subsidence in areas of variable topographic relief: results from analogue modeling, *J. Volcanol. Geotherm. Res.*, *129*, 219–236, doi:10.1016/S0317-0273(03)00241-5.

Macedonio, G., F. Dobran, and A. Neri (1994), Erosion processes in volcanic conduits and application to the AD 79 eruption of Vesuvius, *Earth Planet. Sci. Lett.*, *121*, 137–152.

Marti, J., A. Geyer, A. Folch, and J. Gottsmann (2008), A review on collapse caldera modelling, 233–284 pp., in : Gottsmann, J. & Marti, J. (eds) *Caldera Volcanism: Analysis, Modelling and Response. Developments in Volcanology* Elsevier, Amsterdam.

Marti, J., A. Geyer, A. Folch, and J. Gottsmann (2009), A genetic classification of collapse calderas based on field studies, and analogue and theoritical modelling, 249–266 pp., in: Thordason, T. Self, S. Larsen, G. Rowland, S. K. & Hoskuldosson, A. (eds) *Studies in Volcanology: The Legacy of George Walker* Special Publication of IAVCEI, textbd2.

Massol, H., and T. Koyaguchi (2005), The effect of magma flow on nucleation of gas bubbles in a volcanic conduit, *J. Volcanol. Geotherm. Res.*, *143*, 69–88.

McLeod, P., and S. Tait (1999), The growth of dykes from magma chambers, *J. Volcanol. Geotherm. Res.*, *92*, 231–246.

Michon, L., and F. Massin and V. Famin and V. Ferrazzini and G. Roult (2011), Basaltic calderas: Collapse dynamics, edifice deformation, and variations of magma withdrawal, *J. Geophys. Res.*, *116*, B03209, doi:10.1029/2010JB007636.

Pinel, V., and C. Jaupart (2003), Magma chamber behavior beneath a volcanic edifice, *J. Geophys. Res.*, *108*, (B2) 2072, doi:10.1029/2002JB001751.

Pinel, V., and C. Jaupart (2005), Caldera formation by magma withdrawal from a reservoir beneath a volcanic edifice, *Earth Planet. Sci. Lett.*, *230*, 273–287, doi:10.1016/j.epsl.2004.11.016.

Pinel, V., C. Jaupart, and F. Albino (2010), On the relationship between cycles of eruptive activity and volcanic edifice growth, *J. Volcanol. Geotherm. Res.*, *194*, 150–164,

doi:10.1016/j.jvolgeores.2010.05.006.

Roche, O., T. H. Druitt, and O. Merle (2000), Experimental study of caldera formation, *J. Geophys. Res.*, *105*, 395–416.

Tait, S., C. Jaupart, and S. Vergniolle (1989), Pressure, gaz content and eruption periodicity of a shallow, crystallising magma chamber, *Earth Planet. Sci. Lett.*, *92*, 107–123.

Walter, T. R., and V. R. Troll (2001), Formation of caldera periphery faults: an experimental study, *Bull. Volcanol.*, *63*, 191–203.

Wood, C. A. (1984), Calderas: a planetary perspective, *J. Geophys. Res.*, *89*, 8,391–8,406.

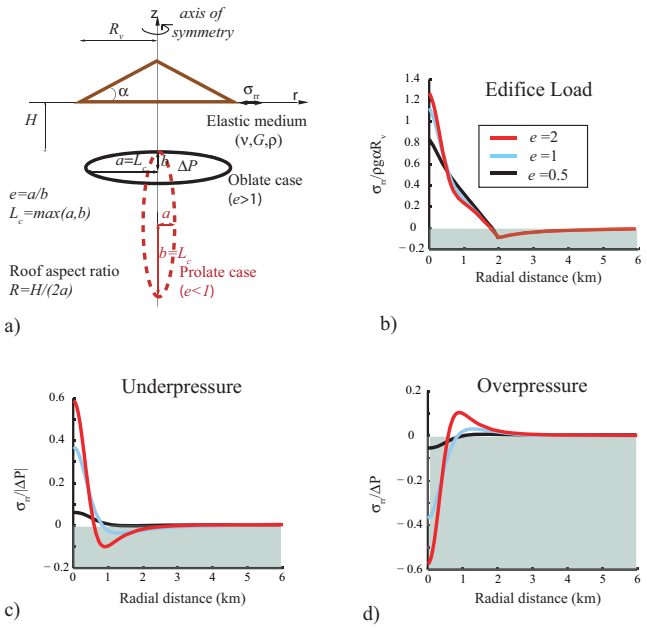

Figure 1. Model geometry and stress field induced at the Earth's surface. a) Model geometry and key parameters. b) Radial stress ($\sigma_{rr}(r)$) induced at the Earth's surface by an edifice load (radius $R_v = 2$ km) when the magma reservoir is at lithostatic equilibrium ($\Delta P = 0$). The stress is normalised by the load applied at the axis. c) Radial stress ($\sigma_{rr}(r)$) induced at the Earth's surface by an underpressurized magma reservoir ($\Delta P < 0$) with no edifice at the surface. The stress is normalised by the magma reservoir underpressure ($|\Delta P|$). d) Radial stress ($\sigma_{rr}(r)$) induced at the Earth's surface by an overpressurized magma reservoir ($\Delta P > 0$) with no edifice at the surface. The stress is normalised by the magma reservoir overpressure (ΔP). Radial stress calculations are obtained for a reservoir depth H of 0.5 km and maximum extension L_c of 0.5 km. Poisson's ratio is equal to 0.25. The black, blue and red curves are obtained, respectively, for a reservoir ellipticity (e) of 0.5, 1 and 2. The grey area corresponds to tensile stress (negative values).

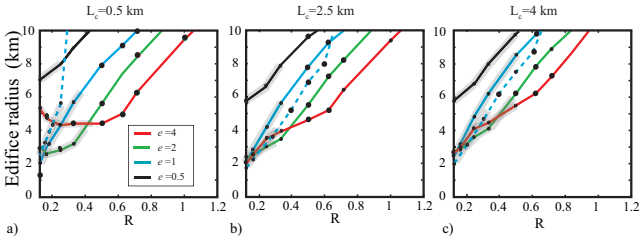

Figure 2. Edifice size required for caldera formation as a function of the roof aspect ratio. The edifice considered is a strato-volcano of slope $\alpha = 0.6$, maximum radius of 10 km and a density of 2800 kgm^{-3}. Poisson's ratio is equal to 0.25 and the rock tensile strength is equal to 200 bars. Results are presented for various reservoir sizes: a) Maximum reservoir extension L_c of 0.5 km, b) Maximum reservoir extension L_c of 2.5 km, c) Maximum reservoir extension L_c of 4 km. Various reservoir ellipticities are considered: the black, blue, green and red curves are, respectively, for a prolate reservoir of ellipticity 0.5, a spherical reservoir, an oblate reservoir of ellipticity 2 and an oblate reservoir of ellipticity 4. The dashed blue curves are analytical results obtained by *Pinel and Jaupart* [2005] for the 2D plane strain case considering a cylindrical magma reservoir. Parts of the curves where the fault linking the Earth's surface rupture location to the reservoir walls is nearly vertical (dip larger than 80 degrees), are surrounded by a grey halo. Black circles are for the numerical simulations performed.

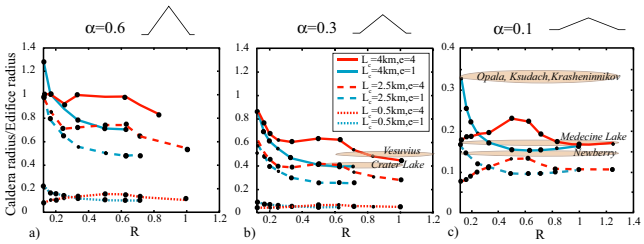

Figure 3. Caldera versus edifice radius as a function of the roof aspect ratio. Two different reservoir ellipticities are considered: the blue and red curves are, respectively, for a spherical reservoir and an oblate reservoir of ellipticity 4. Results are presented for various reservoir sizes: Dotted curves for a maximum reservoir extension L_c of 0.5 km, dashed curves for a maximum reservoir extension L_c of 2.5 km and plain curves for a maximum reservoir extension L_c of 4 km. Poisson's ratio is equal to 0.25 and the rock tensile strength is equal to 200 bars. Volcanic edifice density is 2800 kgm^{-3}. Circles are for the numerical simulations performed. a) The edifice considered is a strato-volcano of slope $\alpha = 0.6$ and maximum allowed size 10 km. b) The edifice considered is a strato-volcano of slope $\alpha = 0.3$ and maximum allowed size 20 km. Characteristics of two strato-volcanoes with a slope close to 0.3, are reported (brown areas): Mount Mazama (caldera/edifice radius close to 0.4 and roof aspect ratio between 0.5 and 1, from [*Pinel and Jaupart*, 2005] and the CCDB) and Vesuvius (caldera/edifice radius close to 0.5 and roof aspect ratio between 0.6 and 1.2, caldera geometry is taken from the CCDB and edifice geometry is estimated from the SRTM Digital Elevation Model). c) The edifice considered is a shield volcano of slope $\alpha = 0.1$ and maximum allowed size 60 km. Characteristics of five shield volcanoes (edifice slope around 0.1) are reported (brown areas): Medecine Lake (caldera/edifice radius close to 0.17), Newberry (caldera/edifice radius close to 0.15), Ksudach, Krasheninnikov and Opala (caldera/edifice radius close to 0.33). Caldera geometry is taken from the CCDB and edifice geometry is estimated from the SRTM Digital Elevation Model.